

# Potential of Femtosecond Electron Diffraction Using Near-Relativistic Electrons from a Photocathode RF Electron Gun

X. J. WANG

*National Synchrotron Light Source, Brookhaven National Laboratory, Upton, NY 11973, USA*

D. XIANG

*Department of Engineering Physics, Tsinghua University, Beijing, China*

T. K. KIM and H. IHEE\*

*Department of Chemistry and School of Molecular Science (BK21),  
Korea Advanced Institute of Science and Technology, Daejeon 305-701*

(Received 20 December 2005)

The electron beam from a photocathode RF electron gun is usually used to drive a free electron laser (FEL) after acceleration and to generate coherent radiation from IR to X-rays. Building on our earlier proposal that such an electron beam itself can be used as scattering particles to produce a time-dependent diffraction signal, which contains structural information on a femtosecond resolution, here we further elucidate several important practical factors relevant to realizing electron diffraction on this time scale. A higher electrical field on the cathode of the RF gun can provide a larger number of electrons per bunch with a shorter temporal width compared to a typical DC gun, owing to a significant reduction in the space-charge effect. The near-relativistic speed of the electrons will further reduce the velocity mismatch and significantly improve the overall time resolution. However, the de Broglie wavelength of near-relativistic electrons at  $\sim 2$  MeV is one order of magnitude shorter than that of the electrons generated by a typical DC gun operated at 30 keV. Consequently the Bragg angle is one order smaller and is comparable to the beam's intrinsic divergence, significantly blurring the observed diffraction pattern. Our simulations show that it is possible to restore the ideal diffraction pattern from the observed, blurred diffraction pattern; therefore, femtosecond electron diffraction using a photocathode RF gun can be a useful and practical tool. In addition, the sensitive dependence of the diffraction pattern on the electron beam divergence can be utilized to measure the divergence with high accuracy.

PACS numbers: 34.50.-s, 29.27.Ac

Keywords: Femtosecond, Electron diffraction, RF gun

## I. INTRODUCTION

X-ray and electron diffraction are two of the most powerful tools for characterizing atomic-scale molecular structure. The development of the electron-storage-ring-based X-ray source and the electron microscope has made it possible to observe matter with Angstrom resolution. On the other hand, the advancement of laser technologies has allowed us to monitor ultrafast processes [1], and molecular dynamics is now studied routinely on picosecond (ps) and femtosecond (fs) time scales by using various spectroscopic methods. However, direct structural information is generally not obtained from such spectroscopic tools and requires a combination of ultrafast spectroscopy [2] and X-ray [3] or electron diffrac-

tion. Examples of this fusion include the X-ray free electron laser (XFEL), now being developed in the U.S. [4] and Germany [5], time-resolved X-ray diffraction [6–12] and time-resolved electron diffraction (TRED) [13–22] for investigating ultrafast structural transitions. Time-resolved diffraction using either an electron or an X-ray pulse is conducted in the pump-probe method: an ultrashort laser pulse is used to initiate a reaction and a diffraction signal from a delayed electron or X-ray pulse probes the progress of the reaction with atomic-scale spatial resolution. Direct observation of fundamental structural transitions, such as bond formation and dissociation, is one of the ultimate goals in scientific fields including nano-science, chemistry, and biology.

X-ray and electron diffraction are complementary techniques. The Thompson scattering cross section is the dominating factor for X-ray diffraction whereas the

\*E-mail: hyotcherl.ihee@kaist.ac.kr; Fax: +82-42-869-2810

Rutherford scattering cross section is that factor for electron diffraction. The difference between X-ray and electron scattering arises from the scattering operator  $L$  [19]:

X-ray diffraction:

$$L_x = \sum_i e^{i\mathbf{s}\cdot\mathbf{r}_i}, \quad (1)$$

Electron diffraction:

$$L_e = \sum_j Z_j e^{i\mathbf{s}\cdot\mathbf{R}_j} - \sum_i e^{i\mathbf{s}\cdot\mathbf{r}_i}. \quad (2)$$

The sums in these formulas span all particles of a molecule.  $\mathbf{s}$  is the momentum transfer vector,  $Z_j$  is the nuclear charge of atom  $j$ , and the distance vectors  $\mathbf{R}_j$  and  $\mathbf{r}_i$  for nucleus  $j$  and electron  $i$ , respectively. It can be seen that the X-ray diffraction signal is the Fourier transform of the electron density distribution within a molecule. The electron diffraction signal is the Fourier transform of the nuclear and the electronic charge distributions. For gas-phase molecule and charge density distribution characterizations, electron diffraction is widely used because its scattering cross-section is six orders of magnitude higher than that of X-rays [23]. Electron diffraction is also relatively compact and less destructive to samples for the same information content.

The temporal resolution of time-resolved electron diffraction (TRED) experiments has been improved by several orders of magnitude over the last decade and has now reached the near sub-picosecond region. Thus, TRED is now a well-established technique [16–18, 20–22] for studying molecular structural changes in chemical reactions. Although this time scale is short enough to study the molecular structure of short-lived and long-lived intermediate species with lifetimes longer than several picoseconds [16], vibrational motions, as well as direct bond-breaking and bond-making processes, [1] cannot be captured. Therefore, the challenge for next-generation TRED is to achieve a femtosecond time resolution (below 100 fs). Toward this goal, we proposed femtosecond electron diffraction using a photocathode RF electron gun [24]. In this contribution, we further elucidate several important practical factors relevant to realizing femtosecond electron diffraction using a photocathode RF electron gun.

In the following section, a discussion of the time resolution of electron diffraction is given. We will then present femtosecond electron beam generation using a photocathode RF gun. Then, we conclude by discussing various issues of femtosecond electron diffraction using a photocathode RF gun.

## II. CHALLENGES IN FEMTOSECOND ELECTRON DIFFRACTION

For a typical TRED experiment, the total time resolution ( $\Delta t$ ) can be expressed as follows:

$$(\Delta t)^2 = (\Delta t_{laser})^2 + (\Delta t_e)^2 + (\Delta t_{VM})^2 + (\Delta t_{jit})^2, \quad (3)$$

where  $\Delta t_{laser}$  is the laser pulse length,  $\Delta t_e$  is the electron pulse (e-pulse) length,  $\Delta t_{VM}$  is the velocity mismatch, and  $\Delta t_{jit}$  is the jitter between the pump laser pulse and the probe e-pulse. Values for  $\Delta t_{laser}$  below 100 fs are now obtained routinely. A typical electron gun (e-gun) can generate sub-ps e-pulses ( $\Delta t_e < 1$  ps) with a significant reduction in the number of electrons [16]. If a good signal-to-noise ratio is to be realized for a gas sample, typically the electron pulse length,  $\Delta t_e$ , has to be longer than 2 ps [16]. The value of  $\Delta t_e$  has been improved by an order of magnitude over the last five years [13] by increasing the electron beam energy in conjunction with reducing the number of electrons and the length of the electron beam path. However,  $\Delta t_{VM}$  is extremely hard to reduce by using present (or similar) e-gun designs based on DC acceleration, where  $\Delta t_{VM}$  is at least a few ps. The  $\Delta t_{VM}$  is caused by the distribution of time delays in the sample due to the difference in speeds between the pump and the probe beams [25].

The value of  $\Delta t_{VM}$  is a function of the sample dimension, the laser beam width, the electron beam (e-beam) width, the geometry of the interaction, and the speed of the e-beam. It can be reduced by either using an e-beam of higher energy, optimizing the geometry, or using a thinner sample. One of the best ways simultaneously to retain a good signal-to-noise ratio and keep  $\Delta t_{VM}$  small (especially in the gas phase) is to increase the speed of the electrons. For a parallel configuration of the laser and the electron-beam and for a sample size on the order of  $\sim 200 \mu\text{m}$ ,  $\Delta t_{VM}$  will be less than 100 fs if the e-beam energy is increased from the current value of  $\sim 30$  keV to more than one MeV. We note that for samples with thin enough thicknesses, such as thin films, the  $\Delta t_{VM}$  may already be sub-picosecond for tens of keV.

Time resolution is not the only limitation of DC acceleration. In the DC configuration, an e-pulse has  $\sim 10^4$  electrons with  $\Delta t_e \approx 4$  ps, which corresponds to  $\sim \text{pA}$  only with a repetition rate of 1 kHz while  $\sim \text{nA}$  currents are easily achieved in conventional CW electron diffraction [16]. Therefore, it is highly desirable to increase the electron flux, thus widening the applicability of the TRED technique. If femtosecond electron diffraction (FED) is to be achieved, two requirements should be met: (a) The kinetic energy should be increased considerably (to at least 1 MeV) to reduce  $\Delta t_{VM}$ . (b) Simultaneously,  $\Delta t_e$  should be reduced significantly ( $\sim 100$  fs) while maintaining (or increasing) the electron flux, which can only be realized by increasing the electron beam's energy.

In the following contribution, we will demonstrate that a photocathode RF gun can satisfy these two conditions. The timing jitter  $\Delta t_{jit}$  between the pump laser and the electron beam must be considered for electron diffraction based on a photocathode RF gun. We will show that it is feasible to achieve a timing jitter below 100 fs with present technologies. Fig. 1 shows a schematic of the experimental set-up for our proposed time-resolved electron diffraction using an RF e-gun. The distortion of the

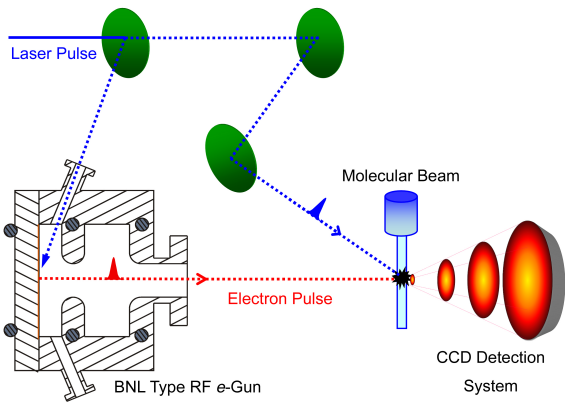


Fig. 1. Schematic of the experimental setup for time-resolved electron diffraction.

laser pulse shape and time slew for an oblique incident angle can be easily corrected with optics although that is not shown in this simplified figure. The transverse distortion can be corrected by using either a cylindrical lens or a pair of prisms, and the time slew can be corrected by using a grating.

### III. FEMTOSECOND ELECTRON PULSE GENERATION BY AN RF GUN

The main factor preventing an increase in flux is the space charge effect caused by the exchange of energy between electrons. The space charge effect is most severe when the density is high, such as near the photocathode. Therefore, a high extraction electric field at the photocathode is most critical. The problem lies in the fact that a typical time-resolved e-gun extracts electrons with a DC field. Currently, the TRED e-gun has an extraction gradient of about 6 MV/m.

The extraction field can be boosted by at least an order of magnitude by using a strong RF field instead of a DC field. Laser driven RF e-guns [26–28] have been developed as potential sources of high-current, low-emittance, short-bunch-length e-beams, which are required for X-ray free electron laser (XFEL) and other applications. In this scheme, the initial electrons are generated in the photocathode and accelerated through an RF-field rather than a DC field. The use of an RF-field alleviates the electrical breakdown limit. Thus, the extraction field can be higher than the DC field. Additionally, the higher extraction field of the RF e-gun suffers less from the space charge effect because the laser-generated electrons in the photocathode are quickly accelerated to near-relativistic speed, thus allowing the generation of an electron flux several orders of magnitude higher than that supplied by e-guns with a DC field.

Another important advantage of using a photocathode RF gun to produce fs e-pulses is its capability of compressing the e-pulse as it is being accelerated in the

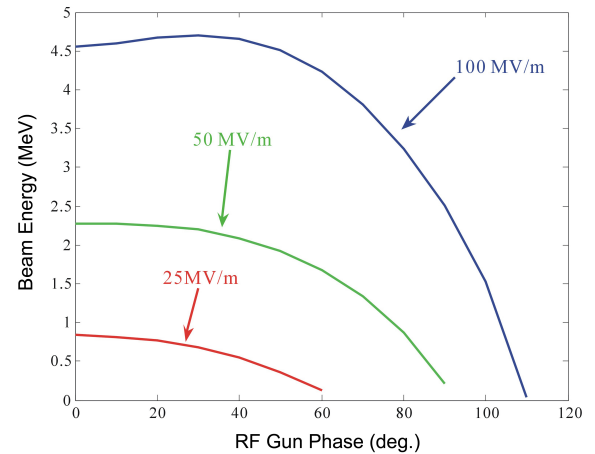


Fig. 2. Photo-electron beam energy vs. RF gun phase for three field gradients.

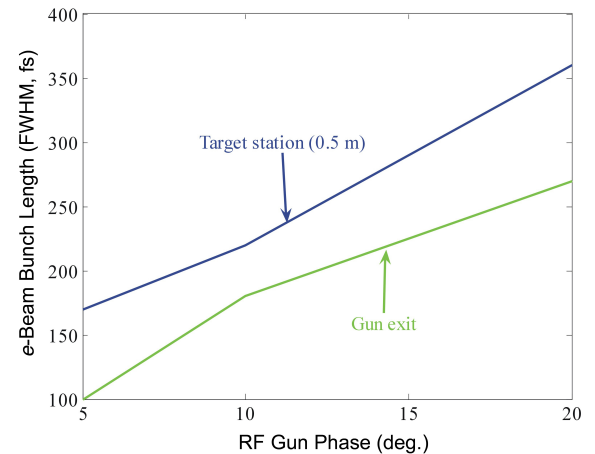


Fig. 3. Photo-electron beam bunch length vs. RF gun phase at the gun exit and the target station.

time-dependent RF field [28]. This permits use of a longer laser pulse and further reduces the space charge effect near the cathode region. Fig. 2 shows the photo-electron beam energy as a function of the RF gun phase and the field gradient on the cathode. By choosing the proper field gradient and RF gun phase, the e-beam energy spread can be minimized. The photocathode RF gun considered here is a 1.6-cell BNL S-band RF gun. In Fig. 3, the electron bunch length at both the RF gun exit and the target station (1 m downstream) is plotted as a function of the RF gun phase for a field gradient of 50 MV/m (2 MeV). The number of electrons for this simulation is approximately  $10^6$ , and the laser pulse length is about 500 fs. Our simulation shows if the number of electrons is reduced to  $10^5$ , the electron bunch length at the target station will be less than 100 fs (FWHM). Table 1 summarizes the expected performance of the photocathode RF gun with a field gradient of 50 MV/m and allows for comparison between it and a typical DC gun.

Besides the improved time resolution, there are other

Table 1. Comparison of femtosecond electron diffraction using DC and RF guns.

	DC gun	RF gun
Time resolution ( $\Delta t$ ) (ps)	$\sim 5$	$< 0.2$
Laser pulse width ( $\Delta t_{laser}$ ) (ps)	$\sim 0.1$	$\sim 0.1$
Electron pulse width ( $\Delta t_e$ ) (ps)	$\sim 4$	$\sim 0.1$
Velocity mismatch ( $\Delta t_{VM}$ ) (ps)	$\sim 2$	$\sim 0.1$
Field on the cathode (MV/m)	DC field ( $\sim 6$ )	RF field (50 – 100)
Electron kinetic energy (MeV)	0.03	1.5 to 4
De Broglie wavelength ( $\text{\AA}$ )	0.066	0.00637 to 0.00277
Speed of electrons	0.33-c	0.86-c to 0.94-c
Camera length	13 cm	A few meters
Divergence (rad)	$10^{-3}$ to $10^{-4}$	$10^{-3}$ to $10^{-4}$
Chromatic coherence length ( $\text{\AA}$ )	33 to 330	10 to 50
Lateral coherence length (lower limit) ( $\text{\AA}$ )	10 to 100	0.4 to 10
Energy spread (%)	0.01 to 0.1	0.005 to 0.01
Number of electrons	$10^4$	$10^5 - 10^6$

advantages of using an RF gun for femtosecond electron diffraction. The electron energy boosted up to at least 1 MeV is capable of deep penetration and allows thicker samples to be studied. This should widen the applicability of time-resolved electron diffraction. In addition, the cost for construction and maintenance are low compared with that for the proposed XFELs because only an RF gun, with no other accelerating components, is needed for femtosecond electron diffraction.

#### IV. PRACTICAL CONSIDERATIONS

The near-relativistic electrons produced by a photocathode RF gun approach the speed of light, resulting in a de Broglie wavelength shorter than that generated by the e-pulses from a 30-keV electron gun. For 2 MeV, the de Broglie wavelength is reduced about 10 times. The scattering intensity is proportional to the square of the de Broglie wavelength. Therefore, the scattering intensity for 2-MeV electrons is about 100 times smaller than that for 30-keV electrons. However, the increased number of electrons for 2 MeV compared with 30 keV compensates for this deficiency. Due to the smaller wavelength, the scattering angle will also be significantly reduced, and the diffraction pattern will be severely contracted into a small detection region. If the same size diffraction pattern is to be recovered, the distance between the interaction volume and the detection screen should be increased from several centimeters to a few meters. Due to the long distance, a devastating problem arises; the diffraction pattern may be highly smeared by the beam's divergence. Thus, the recorded diffraction pattern (RDP) may deviate significantly from the ideal diffraction pattern (IDP) and cannot be directly used for further investigation. Therefore, it is important to study this effect

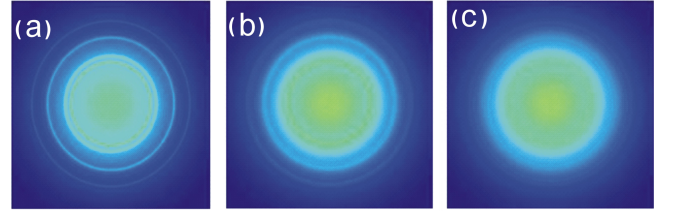


Fig. 4. (a) IDP of polycrystalline Al and the RDP for rms beam divergence of (b) 0.05 mrad and (c) 0.1 mrad.

more systematically and to investigate the feasibility of restoring the IDP from the RDP. To simplify our discussion, we made the following assumptions: First, we assume that the interaction between the electron and the sample does not depend on the incident angle of the electron. Second, the electrons incident upon the sample in different directions are incoherent. Third, the RDP is the IDP for a single electron convoluted with the beam's distribution at the detection plane when the specimen is absent.

The IDP of polycrystalline aluminum and the RDP under the influence of various beam divergences are shown in Fig. 4. The IDP consists of four concentric rings representing the four diffraction planes 111, 200, 220, and 331 with a combination of exponentially decaying backgrounds. The radii of the rings are given by

$$r = \lambda(k^2 + l^2 + m^2)^{1/2}L/a_0, \quad (4)$$

where  $a_0 = 4.05 \text{ \AA}$  is the lattice constant,  $L$  is the distance from the sample to the detector,  $\lambda$  is the De Broglie wavelength of the electron, and  $k$ ,  $l$ , and  $m$  are the Miller indices. As we can see from Fig. 4, the RDPs strongly depend on the beam divergence and deviate significantly from the IDP. Since most of the theory for structure analysis and refinement starts from the IDP, obtaining it from the distorted RDP is necessary. In principle,

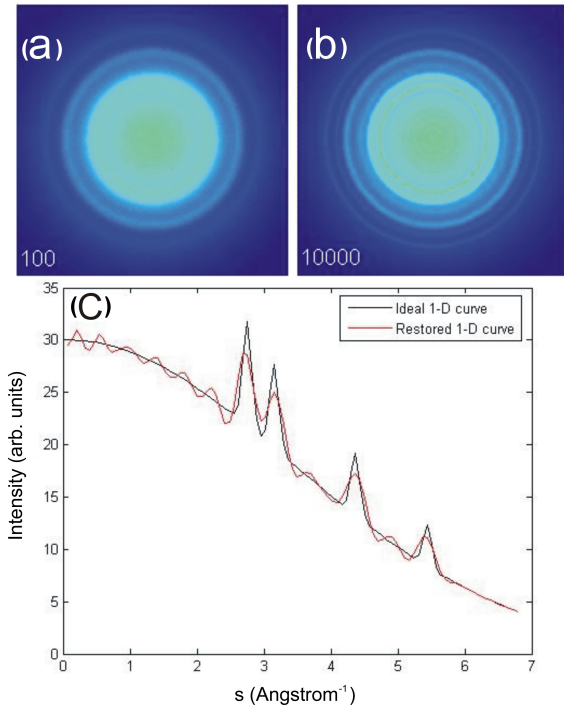


Fig. 5. Restored IDP (a) after 100 iterations, (b) after 10000 iterations. (c) a comparison of the 1-D curve between the IDP and that restored after 10000 iterations.

deconvolution of the RDP should allow retrieval of the IDP, which will be further used for structure investigations. Thus, the effectiveness of the pattern restoration is crucial to the validity of the subsequent ultrafast process study. We have adopted the well-known Richardson-Lucy [29,30] algorithm for pattern deconvolution, instead of a linear inversion algorithm, to take advantage of its intrinsic capability for suppressing noise amplification. The restored IDP for Fig. 4(c) under different iteration numbers is shown in Fig. 5. Fig. 5(c) is a comparison of the 1-D curve between the IDP and that restored after 10000 iterations. The 1-D curve is expressed as a function of  $s$ , the magnitude of momentum transfer between an incident electron and an elastically scattered electron:  $s = \frac{4\pi}{\lambda} \sin \frac{\theta}{2}$ , where  $\theta$  is the scattering angle. The agreement is satisfactory, though not complete. The discrepancy is attributed to the so-called ‘Gibbs phenomenon’ [31], which arises due to finite discrete sampling of the measured data. Actually, any feature in the pattern for which the frequency is beyond that determined by the sampling interval cannot be accurately extracted by deconvolution. Instead, some ‘ringing’ occurs, as can be seen in Fig. 5(c). It is worth pointing out that in our simulation, the IDP is sharper than that obtained by experiments, which indicates that our simulation is quite conservative. For real data, the IDP is smoother due to the finite particle-size and the instrumental-broadening effects, so the high-frequency feature is not so severe, and the restoration, we believe, should be effective and

accurate enough to provide a valid IDP for further investigations.

Besides the smearing of the diffraction pattern by the beam’s divergence, several other new issues also arise when using a photocathode RF gun: lateral incoherence, chromatic incoherence, and timing jitter. First, the lateral incoherence due to the finite size of the electron beam should be considered. For example, if we keep the same camera length of 13 cm for 2-MeV electrons, a beam size of 100  $\mu\text{m}$  corresponds to  $0.96 \text{ \AA}^{-1}$ . Then, the observed diffraction pattern will be a superposition of all diffraction patterns with beam centers over a wide range ( $0.96 \text{ \AA}^{-1}$ ). The net effect would be a reduced diffraction intensity and a shifted phase. Fortunately, one solution is to simply increase the camera length to reduce the ratio of the incident beam size to the diffraction pattern size.

Another important factor is the lateral incoherence due to the finite size of the electron source. The spread of  $s$  due to this effect can be estimated by  $\Delta s = (4\pi/\lambda) \sin(a/2) \approx 2\pi a/\lambda$ , where  $\lambda$  is the de Broglie wavelength and  $a$  is the angle determined by the size of the electron source and the distance between the source and the first pinhole (in the case of an RF gun, this corresponds to the solenoid). The angle is difficult to assess, but the upper limit can be obtained by measuring the divergence of the electron beam. The inverse of this spread corresponds to the lateral coherence length,  $X_L = \lambda/(2\pi a)$ , which roughly estimates the maximum internuclear distance [32,33] that can yield visible diffraction patterns. Since the de Broglie wavelength is about ten times smaller for 2-MeV electrons than it is for 30-keV electrons, to retain the same lateral coherence length,  $a$  has to be reduced accordingly. This adjustment can be achieved simply by placing the first pinhole further away from the electron source at the expense of the electron flux.

Chromatic incoherence is caused by the finite spectral width of the electrons. One can define the chromatic coherence length ( $X_C$ ) as the distance of propagation over which radiation of spectral width  $\Delta\lambda$  becomes out of phase by  $\pi$  radians [34]. Chromatic coherence is estimated from the energy bandwidth  $\Delta n$ , of the electron beam:  $X_C = n_e/(2 \cdot \Delta n) = (\lambda/2) \cdot (\lambda/\Delta\lambda) = (\lambda/2) \cdot (E/\Delta E)$ , where  $n_e$  is the speed of the electron beam. Thus, a larger value for  $X_C$  means greater coherence. The value of  $\Delta n$  for relativistic ultra-short electron pulses is a few orders of magnitude larger than the energy spread of  $\sim 0.4 \text{ eV}$  in typical electron diffraction experiments, but the relative energy spread is comparable at about 0.1 %. The observed diffraction pattern is then a superposition of patterns with frequencies over a wide range, giving an artificial damping of the diffraction signal. If this damping is to be avoided, the energy spread should be reduced to observe the diffraction patterns. The energy spread depends on many factors, such as the temporal width of the laser pulse striking the photocathode, the laser spot size on the photocathode, the initial

and the further broadening due to the space charge effect, and the bunching process. As we pointed out earlier, by properly selecting the field gradient (50 MV/m) and the RF gun phase, an energy spread lower than 0.01 % can be realized, which is comparable to the value for a DC gun. For diffuse scattering from isolated gas molecules, chromatic incoherence is not a serious problem. For example, X-rays with a bandwidth of 2 – 5 % were used successfully to record the diffuse scattering signals from a liquid sample and did not show significant modulation compared to that from monochromatic X-rays [6,35].

For typical pump-probe experiments employed for time-resolved electron diffraction, the timing jitter considered is the arrival-time jitter between the pump laser pulse and the probe electron pulse at the scattering point of the sample. In the experiment, the same laser pulse from a single laser system will be used to generate both the pump laser pulse for initiating reactions in the sample and the other laser pulse for generating electrons from the photocathode RF gun. Therefore, the timing jitter will be the jitter of the e-beam arrival-time at the scattering point. Since the distance traveled by the electrons is constant, the arrival time jitter of the electrons is dominated by the velocity fluctuation, hence, by the energy variation. The energy jitter of the electron beam could come either from the timing jitter between the laser and the RF system or from the RF amplitude fluctuation in the RF gun. Fig. 2 shows that the electron beam energy fluctuation will be less than 0.05 % if the RF gun is operating below 30° and the timing jitter between the laser and the RF clock is less than 1 ps. This corresponds to an arrival time jitter less than 100 fs for a 50-cm travel distance. When the electron beam speed,  $v_e$ , approaches the speed of light,  $c$ , the arrival time jitter,  $\Delta t_{jit}$ , can be approximated by

$$\Delta t_{jit} \approx \frac{l}{c\gamma^2} \left( \frac{\Delta E}{E} \right), \quad (5)$$

where  $\gamma$  is the relativistic factor,  $(1 - v_e^2/c^2)^{-1/2}$ ,  $l$  is the distance from the cathode to the scattering point, and  $(\Delta E/E)$  is the relative energy fluctuation. If the arrival-time jitter is to be kept below 100 fs, not only must the timing jitter between the laser and RF system be kept less than 1 ps, but also the RF amplitude fluctuation must be stabilized better than 0.1 %, which is well within the reach of the present RF technology.

## V. CONCLUSIONS

In summary, use of a photocathode RF gun is suggested as a means to achieve electron diffraction with a time resolution less than 200 fs. The key aspect of femtosecond electron diffraction is the use of a femtosecond electron pulse with a near-relativistic speed along with the high flux out of a laser-driven RF e-gun. The

near-relativistic speed of the electrons will further reduce the velocity mismatch and significantly improve the overall time resolution. Our simulation shows that an RF e-gun can generate 100-fs electron bunches with  $10^6$  electrons. The plausibility of this method was considered, as well as several other factors, such as the lateral and the chromatic coherence lengths relevant to realizing this time scale. The timing jitter between the laser pulse and the electron pulse was shown to be smaller than 100 fs. The use of near-relativistic electrons offers the additional advantage of a longer penetration depth. However, the de Broglie wavelength of near-relativistic electrons, which is one order of magnitude shorter than that of electrons generated by a typical DC gun, makes the Bragg angle one order smaller and comparable to the beam's intrinsic divergence, significantly blurring the observed diffraction pattern. Our simulations show that restoration of the ideal diffraction pattern from the observed, blurred diffraction pattern is possible; therefore, femtosecond electron diffraction using a photocathode RF gun can be a useful and practical tool. In addition, our simulations show that the sensitive dependence of the diffraction pattern on the electron beam divergence can be utilized to measure the divergence with high accuracy.

## ACKNOWLEDGMENTS

For H. I., a preliminary version of this work was formulated during his PhD program under the supervision of Prof. Ahmed Zewail at the California Institute of Technology and was further developed during his postdoctoral program under supervision of Prof. Keith Moffat at the University of Chicago. H. I. acknowledges their guidance and influence. This work was supported by the Korea Science and Engineering Foundation (M2-0520-00-0024-05-B02-00-024-10) and by U.S. Department of Energy, Office of Basic Energy Sciences, under Contract No. DE-AC02-98CH10886.

## REFERENCES

- [1] A. H. Zewail, *Femtochemistry: Ultrafast Dynamics of the Chemical Bond* (World Scientific, Singapore, 1994).
- [2] M. Labardi, M. Allegrini, M. Zavelani-Rossi, D. Polli, G. Cerullo, S. De Silvestri and O. Svelto, *J. Korean Phys. Soc.* **47**, S30 (2005).
- [3] M.-I. Park, C.-O. Park, C. S. Kim and S. C. Jeoung, *J. Korean Phys. Soc.* **46**, 531 (2005).
- [4] J. Galayda, Linac Coherent Light Source (LCLS) Conceptual Design Report, SLAC-R-593, 2002.
- [5] TESLA Technical Design Report Supplement, TESLA-FEL-2002-9, DESY 2002-167, 2002.
- [6] H. Ihee, M. Lorenc, T. K. Kim, Q. Y. Kong, M. Cammarata, J. H. Lee, S. Bratos and M. Wulff, *Science* **309**, 1223 (2005).

- [7] C. Rischel, A. Rousse, I. Uschmann, P.-A. Albouy, J.-P. Geindre, P. Audebert, J. C. Gauthier, E. Forster, J.-L. Martin and A. Antonetti, *Nature* **390**, 490 (1997).
- [8] F. Schotte, M. Lim, T. A. Jackson, A. V. Smirnov, J. Soman, J. S. Olson, G. N. J. Phillips, M. Wulff and P. Anfinrud, *Science* **300**, 1944 (2003).
- [9] I. V. Tomov, D. A. Qulianov, P. Chen and P. M. Rentzepis, *J. Phys. Chem. B* **103**, 7081 (1999).
- [10] C. Rose-Petruck, R. Jimenez, T. Guo, A. Cavalleri, C. W. Siders, F. Raksi, J. A. Squier, B. C. Walker, K. R. Wilson and C. P. J. Barty, *Nature* **398**, 310 (1999).
- [11] C. W. Siders, A. Cavalleri, K. Solkolowski-Tinten, C. Toth, T. Guo, M. Kammler, M. H. V. Hoegen, K. R. Wilson, D. v. d. Linde and C. P. J. Barty, *Science* **286**, 1340 (1999).
- [12] A. Plech, M. Wulff, S. Bratos, F. Mirloup, R. Vuilleumier, F. Schotte and P. A. Anfinrud, *Phys. Rev. Lett.* **92**, 125505 (2004).
- [13] A. A. Ischenko, V. V. Golubkov, V. P. Spiridonov, A. V. Zgurskii, A. S. Akhmanov, M. G. Vabishevich and V. N. Bagratashvili, *Appl. Phys. B* **32**, 161 (1983).
- [14] G. Mourou and S. Williamson, *Appl. Phys. Lett.* **41**, 44 (1982).
- [15] J. D. Ewbank, J. Y. Luo, J. T. English, R. Liu, W. L. Faust and L. Schafer, *J. Phys. Chem.* **97**, 8745 (1993).
- [16] H. Ihee, V. A. Lobastov, U. Gomez, B. M. Goodson, R. Srinivasan, C.-Y. Ruan and A. H. Zewail, *Science* **291**, 458 (2001).
- [17] R. C. Dudek and P. M. Weber, *J. Phys. Chem. A* **105**, 4167 (2001).
- [18] J. Cao, Z. Hao, H. Park, C. Tao, D. Kau and L. Blaszczyk, *Appl. Phys. Lett.* **83**, 1044 (2003).
- [19] I. V. Tomov, P. Chen and P. M. Rentzepis, *J. Appl. Cryst.* **28**, 358 (1995).
- [20] C.-Y. Ruan, V. A. Lobastov, F. Vigliotti, S. Chen and A. H. Zewail, *Science* **304**, 80 (2004).
- [21] C.-Y. Ruan, F. Vigliotti, V. A. Lobastov, S. Chen and A. H. Zewail, *Proc. Natl. Acad. Sci.* **101**, 1123 (2003).
- [22] B. J. Siwick, J. R. Dwyer, R. E. Jordan and R. J. D. Miller, *Science* **302**, 1382 (2003).
- [23] M. H. Pirenne, *The Diffraction of X-rays and Electrons by Free Molecules* (The University Press, Cambridge, 1946).
- [24] X. J. Wang, Z. Wu and H. Ihee, *Femtoseconds Electron Beam Diffraction Using Photocathode RF Gun, Proceedings of the 2003 Particle Accelerator Conference* (Portland, 2003).
- [25] J. C. Williamson and A. H. Zewail, *Chem. Phys. Lett.* **209**, 10 (1993).
- [26] J. S. Fraser, R. L. Sheffield, E. R. Gray and P. M. Giles, *Photocathodes in Accelerator Applications, IEEE Particle Accelerator Conference* (Washington, 1987).
- [27] K.-J. Kim, *Nucl. Instrum. Meth. Phys. Res. A* **275**, 201 (1989).
- [28] K. T. McDonald, *IEEE Trans. Electron Dev.* **35**, 2052 (1988).
- [29] B. H. Richardson, *J. Opt. Soc. Am.* **62**, 55 (1972).
- [30] L. B. Lucy, *Astron. J.* **79**, 745 (1974).
- [31] R. N. Bracewell, *The Fourier Transform and Its Applications* (McGraw-Hill, New York, 1986).
- [32] J. M. Cowley, *Diffraction Physics* (Elsevier, Amsterdam, 1995).
- [33] A. Tonomura, *Electron Holography* (Springer, Berlin, 1998).
- [34] D. Attwood, *Soft X-rays and Extreme Ultraviolet Radiation: Principles and Applications* (Cambridge University Press, New York, 1999).
- [35] A. Plech, R. Randler, G. Armin and M. Wulff, *J. Synchrot. Rad.* **9**, 287 (2002).